Off-Axis Paths in Spherical Mirror Interferometers

D. Herriott, H. Kogelnik, and R. Kompfner

When a spherical mirror interferometer is illuminated by an off-axis ray of light, the repeated reflections cause the ray to trace a path which lies on the surface of a hyperboloid, with the points of reflection on the mirrors on ellipses. Under special conditions, these ellipses may become circles, with the points of reflection displaced by an angle 2θ after every round trip. When $2\nu\theta = 2\mu\pi$, ν and μ being integers, the rays retrace their paths. These ray paths give rise to additional resonances which were observed. Pictures of the points of reflection are reproduced. The theory is in good agreement with the experimental observations. In laser amplifiers these ray paths enable one to obtain long effective path lengths in the active medium which may be contained in a thin annular cylindrical or hyperboloidal shell.

Connes[1] has explored and described the use of a confocal interferometer which consists of two spherical mirrors spaced at a distance equal to twice their focal length. The use of nonconfocal systems as resonators for optical maser oscillators[2,3] leads us to investigate the properties of interferometers formed of spherical mirrors at other than confocal spacings.

If one illuminates an interferometer of this type with a monochromatic light beam from a He–Ne gas maser, for instance, and this beam is misaligned with respect to the interferometer axis, one can measure a free-spectral range which corresponds to an interferometer with a spacing that is several times greater than the actual one. One can also observe an elliptical pattern of spots on each mirror. The number of spots is just equal to the factor by which the apparent interferometer spacing exceeds the actual one.

The patterns of spots and the corresponding resonance characteristics can be explained theoretically in good agreement with experiment.

The ray family inside the interferometer which is obtained in the case of a circular pattern of spots is exactly the one proposed by one of the authors (R. Kompfner) sometime ago as a ray system suitable for optical maser amplifiers.

Distribution of Spots on Mirror Surfaces

In terms of ray optics an interferometer system consisting of two equal and coaxial mirrors is equivalent to a series of equally spaced thin lenses as shown in Fig. 1. The lenses are all of focal length f and they are spaced at distances d.

The authors are with the Bell Telephone Laboratories, Inc., Murray Hill, New Jersey.

Received 15 September 1963.

The behavior of a paraxial ray passing through a system of this kind has been analyzed by Pierce.[4] Using a Cartesian coordinate system, a ray in the section between the nth and the $(n + 1)$th lenses is described by the coordinates (x_n, y_n) of the point where it intersects the center plane of the nth lens, and by the slopes x_n' and y_n' just to the right of this lens (see Fig. 1). We are interested in the coordinates x_n and y_n of a ray which is injected at the input lens with given coordinates x_0 and y_0 and slopes x_0' and y_0'. Using Pierce's results it is easy to show that

$$x_n = x_0 \cos n\theta + \sqrt{\frac{d}{4f - d}}(x_0 + 2fx_0') \sin n\theta, \tag{1}$$

where

$$\cos\theta = 1 - (d/2f). \tag{2}$$

A corresponding relation holds for y_n. We postulate that the lens system is stable, i.e., that

$$0 < \frac{d}{f} < 4 \tag{3}$$

is satisfied.

Equation (1) can be rewritten in the form

$$x_n = A \sin(n\theta + \alpha), \tag{4}$$

with

$$\tan\alpha = \sqrt{\frac{4f}{d} - 1} \Big/ \left(1 + 2f\frac{x_0'}{x_0}\right) \tag{5}$$

and

$$A^2 = \frac{4f}{4f - d}(x_0^2 + dx_0x_0' + dfx_0'^2). \tag{6}$$

The quantity A is the maximum possible excursion of the ray in the x direction, on its way through the series of lenses for given initial values x_0 and x_0'.

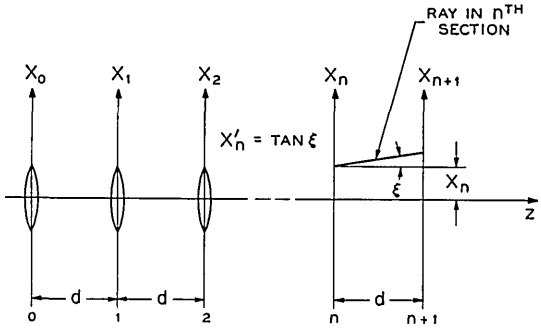

Fig. 1. Series of equally spaced thin lenses.

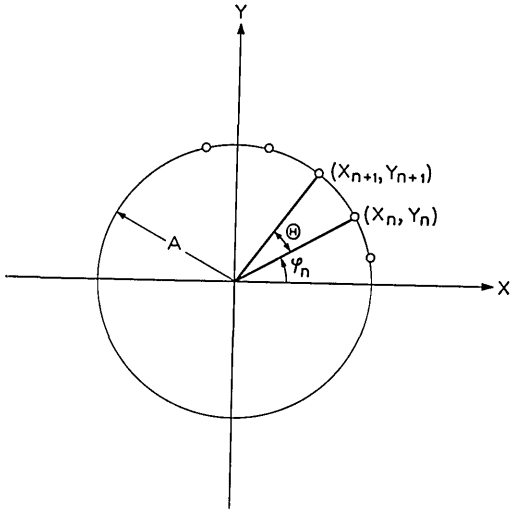

Fig. 2. Projections of intersection points (x_n, y_n) lying on circle.

For the y coordinate one obtains similarly

$$y_n = B\sin(n\theta + \beta). \tag{7}$$

Imagine, now, all intersection points (x_n, y_n) for a given ray projected into an x–y plane. We can see from Eqs. (4) and (7) that these projections will, in general, lie on an ellipse. In special cases they will be on a circle, namely, when

$$A = B \tag{8}$$

and

$$\alpha = \beta \pm \frac{\pi}{2} \text{ (or } \tan\alpha \cdot \tan\beta = -1). \tag{9}$$

A is, of course, the radius of the circle.

Equations (8) and (9) impose certain conditions on the initial values x_0, y_0, x_0', and y_0'. If we postulate, for instance, that $y_0' = 0$ and prescribe x_0, then y_0, the radius A, and the slope x_0' are determined via Eqs. (4) and (5):

$$y_0^2 = x_0^2\left(\frac{4f}{d} - 1\right), \tag{10}$$

$$A^2 = x_0^2 + y_0^2 = \frac{4f}{d}x_0^2, \tag{11}$$

$$x_0' = -\frac{2x_0}{d} = -\frac{A}{\sqrt{fd}}. \tag{12}$$

This last relation tells us with what slope the ray has to be injected to produce a desired circle of radius A.

In Fig. 2 the projections of the intersection points (x_n, y_n) on an x–y plane are shown for the case where they lie on a circle. Under this condition the polar angle φ_n corresponding to the point (x_n, y_n) is

$$\varphi_n = n\theta + \alpha. \tag{13}$$

The difference in polar angle between this point and its neighbors (x_{n+1}, y_{n+1}) is therefore equal to the angle θ which was defined in Eq. (2) for mere analytical reasons.

We can use the above findings to understand the way in which a ray is reflected back and forth between the two concave mirrors of a resonator. The even-numbered intersection points will be the points where the ray strikes the one mirror, and the odd-numbered points will correspond to the points of impact on the other mirror.

If the ray is injected at the angle given by Eq. (12), the points of impact on each mirror will lie on a circle, and the difference in polar angle between neighboring points on one particular mirror will amount to 2θ. While it is reflected back and forth between the two mirrors, the ray stays on the surface of a rotational hyperboloid. This fact can be used in designing a maser amplifier, where the rays use the volume of a concentric cylindrical shell.

In particular, it has been found that the gain and power output of an optical maser, employing a gas as the active medium, depends critically on the distance between the light rays and the walls containing the gas. The proposed system of rays enables one to construct an annular container having walls sufficiently close to all the rays and having, because of its cylindrical geometry, sufficient mechanical strength to withstand the pressure difference between the gas and the atmosphere.

The mirror system has, of course, all the refocusing properties of a periodic sequence of lenses. To keep all spots as small as possible it is necessary to image the beam so that the wavefront has the same curvature as the illuminated mirror surface and to limit its aperture to the diameter of the fundamental cavity mode at the surface of the mirror.

Photographs of the distribution of spots on one of the mirror surfaces were taken when the spherical surface cavity was illuminated with the beam from a He–Ne maser.

The mirrors used in the cavity were slightly transparent, so a field lens was placed just beyond the mirror to collect the transmitted light into a camera lens which was used to image the spots onto polaroid photographic film. The mirrors were changed to ob-

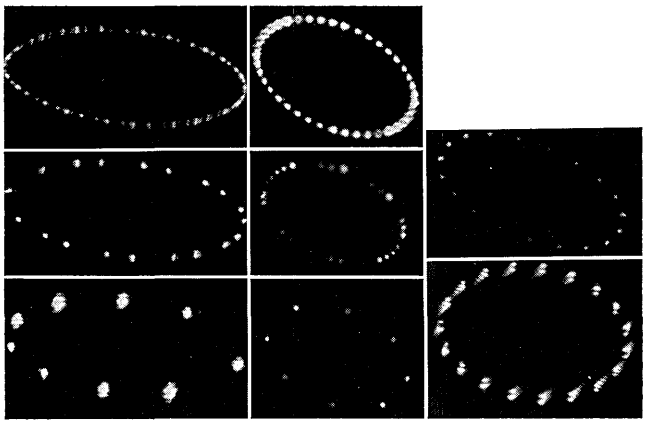

(a) (b) (c)

Fig. 3. Photographs of light patterns on mirrors.

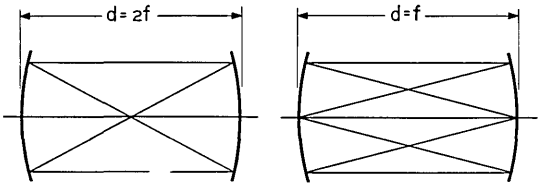

Fig. 4. Closed ray paths.

tain various cavity geometries, and a series of pictures as shown in Fig. 3 was obtained.

Re-entrant Condition

If the resonator dimensions are such that 2θ is an integer fraction ν of 2π, namely,

$$2\nu\theta = 2\pi, \tag{14}$$

then a ray returns exactly to its entrance point $(x_0, y_0) = (x_\nu, y_\nu)$ after ν return trips through the system, and continues to retrace the same ray pattern again and again. Closed paths of this type are known to exist for the confocal resonator with a repetition rate of two return trips as shown in Fig. 4(a). For a system with a mirror separation equal to the focal length ($d = f$), one has a closed path of three basic return trips. This is shown in Fig. 4(b). Other "magic" resonator dimensions can be computed from Eqs. (2) and (14), some of which are given in the following table:

ν	2	3	4	6	12	24
f/d	0.5	1	1,7	3,7	14,7	58

It is only the ratio between focal length and mirror spacing which determines whether one has a closed path or not. It can be seen from Eq. (1) that, if condition (14) holds, a ray returns to its entrance point after ν return trips no matter what its entrance slope. To obtain a closed path it is, therefore, not necessary that the points where the ray strikes one of the two mirrors lie on a circle. Equations (1) and (14) tell us, in addition, that one obtains a 1:1 image of the input spot after ν return trips (and an inverted image after $\nu/2$ return trips if ν is even). The radiation does not spread as in free space but is continuously refocused by the concave mirror system.

More complicated closed ray paths are obtained when

$$2\nu\theta = 2\mu\pi$$

with μ an integer number, not equal to ν.

An examination of the pictures in Fig. 3 shows that the number of spots is due to repeated circuits around the ellipse. By inserting a blade into the space between the mirrors, it is possible to intercept the beam after only one pass around the ellipse and to show the distribution of spots in one circuit.

Figure 3(a) shows the intersection at one mirror of an off-axis path between a 2-m radius reflector and a 10.5-m radius reflector at a spacing of 14.6 cm. The lower picture shows the path interrupted after nine multiple reflections or one complete circuit of the ellipse. The center picture shows the pattern on one reflector when the beam is limited to two circuits of the ellipse consisting of 19 multiple reflections. The upper picture shows the pattern resulting from unlimited multiple reflections in the resonator. Figure 3(b) shows the same patterns for mirrors of 2-m radius at 14.6-cm spacing. It can be seen that the ray becomes re-entrant after five circuits of the ellipse made up of 40 multiple passes between the mirrors. Picture 3(c) shows the patterns for one circuit and unlimited passes in a resonator with 10.5-m mirrors at 14.6-cm spacing.

To discuss the interferometric properties of our configuration assume that both mirrors have a power reflection coefficient R and a transmission coefficient T and that a light beam suffers a phase shift φ during transit from one mirror to the other.

If a light beam is injected in perfect alignment with the optic axis of the mirror system (interferometer), interference will take place after each return trip of the light beam, and one observes the well-known[5] characteristics of a Fabry–Perot interferometer:
a transmission T_0 given by

$$T_0 = \frac{T\, e^{j\varphi}}{1 - Re^{2j\varphi}}, \tag{15}$$

a fringe finesse

$$F_0 = \frac{\pi\sqrt{R}}{1 - R}, \tag{16}$$

and a cavity Q factor

$$Q_0 = \frac{\varphi}{1 - R}. \tag{17}$$

Considering the case where the beam is injected at an angle of off-axis, let us assume that the interfero-

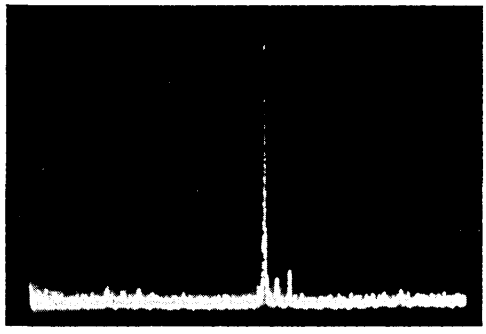

(a)

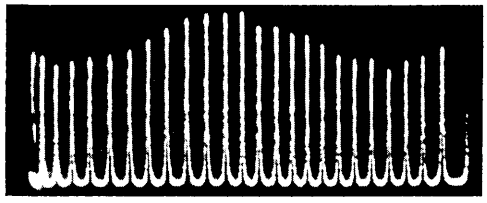

(b)

Fig. 5. Spectra of spherical mirror resonator. (a) Axial illumination. (b) Off-axis illumination.

meter dimensions are such that we have a closed path of ν return trips and that the spots of beam impact on each mirror do not overlap. Interference will now take place only after ν return trips, and the spectral response of this configuration will be similar to a Fabry–Perot of ν times the mirror spacing. It is easy to show that the power transmission T_ν through the first output spot is given by

$$T_\nu = \frac{T\, e^{j\varphi}}{1 - R^\nu\, e^{2j\nu\varphi}}, \tag{18}$$

the fringe finesse by

$$F = \frac{\pi R^{\nu/2}}{1 - R^\nu}, \tag{19}$$

and the Q factor by

$$Q = \frac{\nu\varphi}{1 - R^\nu}. \tag{20}$$

If we compare this to the original one-return-trip interferometer, we notice that for reflectivities close enough to unity the finesse has deteriorated by a factor ν and the Q factor only slightly improved.

Resonances of a Spherical Interferometer

The resonances of the interferometer were examined with an oscillating interferometer[6] in which the spacing between the two mirrors was varied sinusoidally at 60 cps over a distance of about a wavelength permitting the transmitted band to be scanned in wavelength. The interferometer was illuminated with the beam from a He–Ne maser, and the transmitted light was received by a multiplier phototube and displayed on an oscilloscope. The sweep of the oscilloscope was driven in synchronism with the drive of the mirror spacing.

When this interferometer was illuminated on the axis of the interferometer, patterns, as shown in Fig. 5(a), were obtained showing the detail of the output of the maser. When the interferometer was illuminated in an off-axis manner, the single resonant peak of the cavity was broken up into nineteen resonances, as shown in Fig. 5(b). Their individual amplitudes are still modified by the original resonant period. These nineteen resonant peaks within the width of the usual spacing correspond to the nineteen round trips through the interferometer before the beams are reentrant.

Conclusions

An examination of ray paths in a nonconfocal spherical interferometer shows that off-axis paths have interesting properties which may, on the one hand, be of use in amplifiers and absorption cells and which, on the other hand, may adversely affect the performance of an interferometer.

References

1. P. Connes, Rev. Opt. **35**, 37 (1956); J. Phys. Radium **19**, 262 (1958).
2. G. D. Boyd and J. P. Gordon, Bell System Tech. J. **40**, 489 (1961).
3. G. D. Boyd and H. Kogelnik, Bell System Tech. J. **41**, 1347 (1962).
4. J. R. Pierce, *Theory and Design of Electron Beams* (Van Nostrand, New York, 1954), pp. 194–197.
5. M. Born and E. Wolf, *Principles of Optics* (Pergamon, New York, 1959), 322–332.
6. D. R. Herriott, Appl. Opt. **2**, 865 (1963).